TISSUE ENGINEERING: Part A
Volume 15, Number 10, 2009

DOI: 10.1089/ten.tea.2008.0502

Original Article

Cell-Induced Alignment Augments Twitch Force in Fibrin Gel–Based Engineered Myocardium via Gap Junction Modification

Lauren D. Black III, Ph.D.,[1] Jason D. Meyers, M.D.,[1] Justin S. Weinbaum, Ph.D.,[1] Yevgeniya A. Shvelidze, B.S.[1] and Robert T. Tranquillo, Ph.D.[1,2]

A high-potential therapy for repairing the heart post-myocardial infarction is the implantation of tissue-engineered myocardium. While several groups have developed constructs that mimic the aligned structure of the native myocardium, to date no one has investigated the particular functional benefits conferred by alignment. In this study we created myocardial constructs in both aligned and isotropic configurations by entrapping neonatal rat cardiac cells in fibrin gel. Constructs were cultured statically for 2 weeks, and then characterized. Histological staining showed spread cells that express typical cardiac cell markers in both configurations. Isotropic constructs had higher final cell and collagen densities, but lower passive mechanical properties than aligned constructs. Twitch force associated with electrical pacing, however, was 181% higher in aligned constructs, and this improvement was greater than what would be expected from merely aligning the cells in the isotropic constructs in the force measurement direction. Our hypothesis was that this was due to improved gap junction formation/function facilitated by cell alignment, and further analyses of the twitch force data, as well as Western blot results of connexin 43 expression and phosphorylation state, support this hypothesis. Regardless of the specific mechanism, the results presented in this study underscore the importance of recapitulating the anisotropy of the native tissue in engineered myocardium.

Introduction

Cardiovascular disease is one of the leading causes of death in the United States[1] and while there are currently a number of therapies aimed at preventing or treating heart failure post-myocardial infarction, none of these treatments result in the replacement or regeneration of infarcted myocardial tissue. Indeed heart transplantation remains the last treatment option with good long-term results[2]; however, there is a persistent critical shortage of donor hearts available, even as the incidence of cardiovascular disease and heart failure continues to rise. The result is a growing need for new and innovative therapies to mitigate heart failure. One such therapy is the use of tissue engineering principles to create a functional myocardial tissue graft *in vitro*.

Several distinct strategies to develop three-dimensional contracting myocardial equivalents (MEs) *in vitro* currently exist, including seeding preformed synthetic or biologic matrices,[3–6] the stacking of two-dimensional monolayers of cardiac cells,[7] and entrapping cardiac myocytes in biologic gel–fiber networks.[8,9] While each of these methods has resulted in contractile tissue, they all fail to explore the importance of alignment of the cells and the extracellular matrix (ECM). Native myocardium consists of layers of aligned myocytes and matrix fibers leading to a large degree of mechanical and electrical anisotropy. Studies on native tissue have found that this anisotropy is an important component of the functional performance of myocardium,[10,11] and it has been recently argued that recreating this anisotropy should be a critical design criterion of engineered myocardium.[12,13] While some groups have created aligned tissue constructs either through mechanical stimulation during culture,[8] via coculture with cardiac fibroblasts,[6] or via constrained self-assembly techniques,[9,14] to date no one has investigated how much or why this anisotropy improves tissue function. Our hypothesis is that cell and matrix alignment of MEs results in an improvement in twitch force over isotropic tissue that is greater than expected by merely aligning all the cells in the direction of force measurement; further, this augmented improvement is due to the cells being organized into an interconnected network resulting in better electromechanical function. Potential reasons for this increased twitch force could be improvements in gap junction expression, gap junction function, or force transmission through the ECM in aligned constructs.

The goal of this study was to evaluate the impact of cell and matrix alignment on tissue function in engineered

Departments of [1]Biomedical Engineering and [2]Chemical Engineering, University of Minnesota, Minneapolis, Minnesota.

myocardium. We created MEs by entrapping neonatal rat cardiac cells in a fibrin gel. The advantage of fibrin as a biological scaffold is that the cells are more likely to remodel the fibrin matrix and replace it with their own ECM as compared to collagen gels.[15,16] By appropriately constraining the cell-induced fibrin gel contraction, the fibrin fibrils align and then the cells align in the same direction via a hypothesized contact guidance response.[17] The result is an aligned ME containing aligned ECM produced by the cardiac cells, the result of the cells replacing the fibrin with their own ECM. To study the consequences of alignment, we created both aligned and isotropic constructs and compared their morphology, passive mechanical properties, and twitch force. Our results show that alignment results in an improvement in twitch force that is greater than what could be expected from merely aligning the cells in the direction of force measurement, and this improvement correlated with changes in the overall expression and phosphorylation state of connexin 43 as analyzed via Western blot.

Materials and Methods

Culture of aligned and isotropic constructs

Constructs were made by adding freshly isolated mixed cardiac cells from 2-day-old neonatal Sprague-Dawley rats at a final concentration of 5×10^6 cells/mL with a fibrin-forming solution comprised of bovine fibrinogen 5 mg/mL, bovine thrombin 2 U/mL, and 2 M $CaCl_2$. The resulting constructs had an initial volume of ~1.25 mL and a final fibrin concentration of 3.3 mg/mL. Constructs were cast into tubular molds and created in both aligned ($n=18$) and quasi-isotropic ($n=18$) configurations using adherent (bare Teflon) or nonadherent mandrels (Teflon coated with 2% agarose) as previously described.[18] In both configurations, after the molds were injected with the fibrinogen–cell mixture, they were incubated for 20 min at 37°C to allow the fibrin gel to form. Once set, the constructs were placed in jars containing culture medium (Dulbecco's modified Eagle's medium, 10% fetal bovine serum, 1% Pen-Strep, aminocaproic acid [to a final concentration of 6 mg/mL]—to control fibrinolysis, TGF-β [1 ng/mL; R&D Systems Inc., Minneapolis, MN], insulin [2 μg/mL; Sigma-Aldrich], and ascorbic acid [50 μg/mL; Sigma-Aldrich Corporation, St. Louis, MO]—all to promote ECM production) and cultured for 14 days with a complete medium change every other day. The isotropic constructs (adherent mandrels) contract in the circumferential and radial directions, while the aligned constructs (nonadherent mandrels) also contract in the axial direction, resulting in a shorter but circumferentially aligned tubular construct. The degree of alignment of the matrix fibers of the constructs was characterized using a polarized light imaging technique previously developed.[19] To determine cellular alignment, whole constructs were stained with phalloidin stain for F-actin, similar to the recent study by Nichol *et al*.,[6] and imaged on a confocal microscope (Olympus Corporation Fluoview 1000 IX2, Tokyo, Japan).

Histology and immunohistochemistry

Constructs were fixed in 4% paraformaldehyde, frozen in embedding medium (Tissue-Tek, OCT; Sakura-Finetek U.S.A. Inc., Torrance, CA), cut with a cryostat into 10 μm sections at −20°C, and placed onto Superfrost/Plus microscope slides (ThermoFisher Scientific Inc., Waltham, MA). All slides were then stained or labeled with fluorescent antibodies and imaged in epifluorescence. To evaluate the ECM organization, Lillie's Trichrome stain (Sigma-Aldrich Corp. St. Louis, MO) was used. Sections were also labeled with a marker for cardiac myocytes, myosin heavy chain (MHC) (Cat#: sc-32732; Santa Cruz Biotechnology Inc., Santa Cruz, CA). In addition, the cardiac fibroblasts were labeled with smooth muscle α-actin (SMA) (Cat#: ab18147; Abcam Inc., Cambridge, MA). In all fluorescent images cell nuclei were labeled with a DAPI stain (Vectashield Mounting Medium; Vector Laboratories Inc., Burlingame, CA). Finally, construct sections were stained with a TUNEL assay (Promega Corporation, Madison, WI) to assess apoptotic cells.

Characterization of cellularity

Final cellularity of all constructs was quantified using a DNA assay as previously described.[20] In addition, cellular composition of the constructs after 2 weeks was assessed by recovering the cells via collagenase digestion on a small subset of samples ($n=4$ for each group). The recovered cells were fixed in suspension and labeled with the MHC antibody described above and counted via FACS analysis (PCA-96; Guava Technologies Inc., Hayward, CA) to determine the final percentage of myocytes in the two construct types.

Measurement of passive mechanical properties

Constructs were attached to a Micro Bionix uniaxial testing machine (MTS Systems Corporation, Eden Prairie, MN) via custom-made clamps and submerged in phosphate buffered saline (Mediatech Inc., Manassas, VA) at 25°C. The direction that was strained was the circumferential direction of the tubes (i.e., the direction of alignment for aligned constructs). All constructs underwent six quasi-static tensile tests to 40% strain (sample preconditioning), followed by a quasi-static strain-to-failure test (1% strain/s). Tangent modulus of the constructs was determined as the slope of the linear portion of the failure test. In addition, the ultimate tensile strength (UTS), defined as the maximum stress achieved before failure, was recorded.

Construct biochemical composition

The ECM composition of all constructs was quantified by conducting assays for total protein, elastin, and hydroxyproline content—a surrogate for collagen content. The assay for determining hydroxyproline was adapted from the method used by Stegemann *et al*.[21] To determine elastin and total protein content, a Ninhydrin-based assay adapted from Starcher *et al*. was used.[22]

Twitch force measurements

Twitch force was measured using a custom-built testing system. To ensure synchronous contraction the constructs were paced via general field stimulation using a cardiac stimulator (S88×; Astro-Med Inc., West Warwick, RI). Twitch force was recorded at a preload of 10 mN in response to a 1 Hz pulse train of 10 ms long, monopolar square waves with amplitudes of 8 V/cm. Data were acquired using a custom-made LabVIEW algorithm (National Instruments Corpora-

tion, Austin, TX) and analyzed offline using Matlab (The Mathworks Inc., Natick, MA). Twitch force was defined as the peak force achieved during pacing minus the baseline force immediately before the pacing stimulus. Values for each construct were the average twitch force of 10 pacing events after the twitch force had reached steady state.

Western blot

Western blot analysis was conducted on a smaller set of constructs ($n = 6$ for both groups). Briefly, portions of each construct were lysed by sonication in ice-cold lysis buffer (25 mM Tris [pH 7.4], 225 mM NaCl, 25 mM NaF, 5% glycerol, 0.5% Nonidet P-40, 0.025% sodium deoxycholate, 1 mM EDTA, 2 mM $NaVO_4$, 1 μg/mL aprotinin, pepstatin, and leupeptin; Sigma-Aldrich), and the total protein of the resulting lysate was analyzed using a BCA total protein assay (Pierce Biotechnology Inc., Rockford, IL). The results of this assay were used to load the lanes of the polyacrylamide gels with 20 μg of protein, and a Western blot was conducted using primary antibodies to evaluate the expression of the following proteins in aligned and isotropic constructs: the gap junction protein connexin 43 (Cx43, Cat#: C8093; Sigma-Aldrich), the expression of Cx43 that is phosphorylated at residue serine 368 (pCx43s368, Cat#: 3511; Cell Signaling Technology Inc., Beverly, MA), and the calcium storage molecule calsequestrin-2 (Csq2, Cat#: C3868; Sigma-Aldrich). Blots were blocked with 3% bovine serum albumin (Sigma-Aldrich) in tris-buffered saline, and appropriate horseradish-peroxidase-conjugated secondary antibodies (all from Jackson Immunoresearch Laboratories Inc., West Grove, PA) were used to label blots for enhanced chemi-luminescence assay. Expression intensities were analyzed using Image J (NIH). Detailed methods for the Western blotting technique were previously described.[23]

Statistical analysis

All results were compared using Student's *t*-test with significance determined as $p < 0.05$.

Results

Creation of aligned and isotropic constructs

Figure 1 shows an isotropic construct (A) and aligned construct (B) after 2 weeks of culture. The aligned construct has contracted to a thin ring in the center of the length of the mandrel (white arrow). After 2 weeks in culture there was a significant difference between aligned and isotropic construct thickness (aligned: 290.5 ± 37 μm, isotropic: 73.2 ± 18.3 μm, $p < 0.001$) and axial length (aligned: 2.37 ± 0.37 mm, isotropic: 8.36 ± 1.37 mm, $p < 0.001$), but not construct volume (aligned: 20.12 ± 3.31 mm^3, isotropic: 19.17 ± 8.28 mm^3, $p = 0.714$). Matrix alignment, or lack thereof, was verified by polarized light imaging for both the isotropic (C) and the aligned (D) configurations. In these images the grayscale intensity represents the pixel-wise retardation values, while the lines (black in Fig 1C, white in Fig 1D) indicate the local average direction of alignment and their length indicates the local average retardation. Since retardation is indicative of strength of alignment, note that the aligned construct is highly aligned in circumferential direction while the isotropic construct shows no preferential alignment. Cellular alignment (E, F), as assessed by F-actin staining on whole constructs, matched matrix alignment for both construct types.

Histology and immunohistochemistry

In the sections stained with Lillie's Trichrome (Fig. 2 top row), a layer of collagen was evident on the side in contact with the medium in both construct types (blue-green color), and the aligned constructs displayed elongated nuclei in the circumferential direction. Images from each construct type with antibodies for MHC to detect myocytes (Fig. 2 second row), and SMA to detect fibroblasts (Fig. 2 third row) are shown. In both construct types, cells exhibited the striated pattern of MHC associated with cardiac muscle (see 60× MHC image for each construct type). In addition, there were a significant number of cells that stained positively for SMA, which presumably represent both smooth muscle cells and cardiac fibroblasts. Finally, TUNEL staining on sections from both construct types (Fig. 2, bottom row) showed increased apoptotic cells in the aligned constructs as compared to the isotropic constructs.

Cellular content

Figure 3A displays the results of DNA quantification of both aligned and isotropic constructs after 2 weeks in culture. In both geometric configurations there was a large cell loss over the 2-week culture period (initial cell number: 5×10^6). In addition, isotropic constructs had a 132% higher final cell number than aligned constructs as estimated from the DNA quantification ($p < 0.04$). Final cellular concentrations were $4.57 \times 10^7 \pm 2.18 \times 10^7$ cells/cm^3 for the aligned constructs and $1.04 \times 10^8 \pm 3.04 \times 10^7$ cells/cm^3 ($p < 0.01$) for the isotropic constructs. FACS analysis ($n = 4$ for each group) of cells recovered from the constructs after 2 weeks in culture showed that the percentage of MHC-positive cells was significantly higher ($p < 0.01$) for aligned constructs ($54.6 \pm 8.4\%$) as compared to isotropic constructs ($33.0 \pm 6.5\%$).

Passive mechanical properties

The passive mechanical properties during strain-to-failure tests were measured (Fig. 3B). As expected, both the UTS and the tangent modulus of the aligned constructs were greater than those of the isotropic constructs ($p < 0.01$ in both cases).

Biochemical composition

Total protein and collagen content were measured after 2 weeks in culture (Fig. 3C, D). The total protein density was 27% higher in the isotropic constructs ($p < 0.04$). In addition, the collagen density was 215% higher in the isotropic constructs ($p < 0.0001$).

Twitch force

Both construct types displayed spontaneous contractions of between 2 and 3 Hz (see Supplemental Video, available online at www.liebertonline.com). An example of the twitch force as a function of time for 1 Hz pacing is shown for an aligned construct in Figure 4A and an isotropic construct in Figure 4B. The average twitch force for aligned and isotropic constructs paced at 1 Hz is presented in Figure 4C. The force

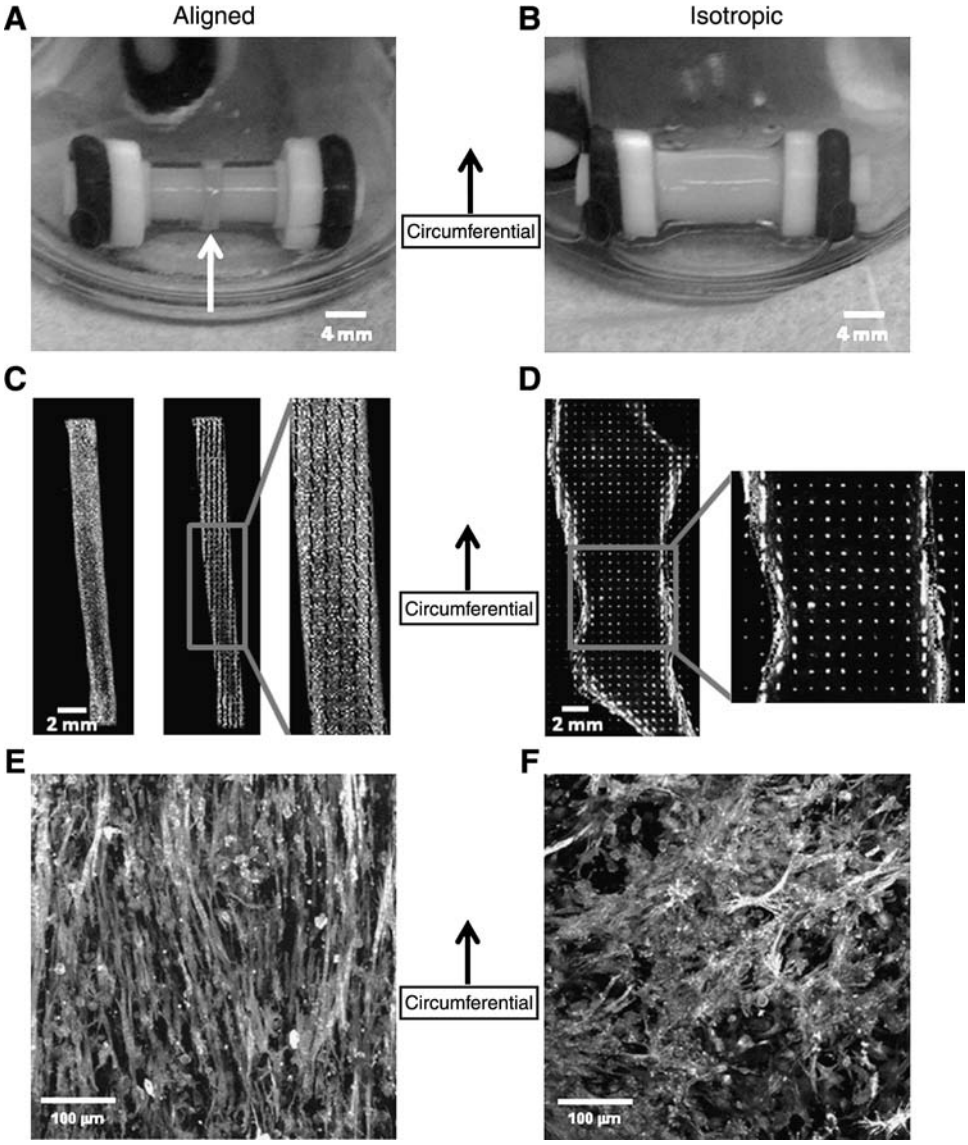

FIG. 1. Images of isotropic (**A**) and aligned (**B**) constructs after 14 days in culture with corresponding polarized light alignment images (**C, D**). In (**C, D**) the constructs have been cut axially and splayed flat. The grayscale values represent the birefringence of the tissue, a measure of the strength of alignment, and the lines (black in **C**, white in **D**) indicate the local average direction of alignment in the tissue. Note that the aligned construct (**D**) is highly aligned in the circumferential (vertical) direction, while the isotropic construct (**C**) does not possess alignment. Cellular alignment, measured via staining of filamentous actin, matched matrix alignment assessed via polarized light for both construct types (**E, F**).

for aligned constructs is around 1.3 mN, as compared to 0.47 mN for the isotropic constructs ($p < 10^{-5}$).

Western blot analysis

Representative blots of connexin 43 (Cx43), connexin 43 phosphorylated at residue Serine 368 (pCx43s368), calsequestrin-2 (Csq2), and β-actin are shown for two aligned (A_1, A_2) and two isotropic (I_1, I_2) constructs in Figure 5A. The double banding of the Cx43 blot at 44 and 46 kDa represents the different phosphorylation states of Cx43. The intensities for each antibody were grouped by construct type and compared statistically ($n = 6$ for both groups). Figure 5B displays the ratio of pCx43s368 expression to the total Cx43 expression for the aligned and isotropic constructs. These results indicate that there was a greater percentage of pCx43s368 in isotropic as compared to aligned constructs ($p < 0.05$). In addition, there was a greater expression of Csq2 in the aligned constructs (4587 ± 1020 for aligned vs. 3316 ± 1003 for isotropic, $p < 0.05$). These data mirror the findings from the FACS analysis that showed that the aligned constructs contained a higher percentage of MHC-positive cells after 2 weeks of culture. Isotropic constructs had a 52% higher ratio of Cx43/Csq2 (Fig. 5C, $p < 0.04$) and an 85% higher ratio of pCx43s368/Csq2 (Fig. 5D, $p < 0.02$).

Discussion

The creation of engineered myocardium *in vitro* is a topic that has garnered significant interest in recent years and has led to a wealth of studies using different fabrication and culture techniques. The goal of this study was to investigate the consequences of cell alignment on tissue morphology, passive mechanical properties, and twitch force of fibrin gel-based MEs. While our method for creating MEs results in functional engineered myocardium, there still exist several issues. One issue is cell viability in MEs after 2 weeks in culture. The results presented in Figure 3A show that after 2 weeks in culture only 18–40% of the cells initially entrapped in the gel remain. Since the myocyte is a very metabolic cell, this cell loss could be due to the fact that the MEs are cultured statically with diffusion being the sole mode of nutrient

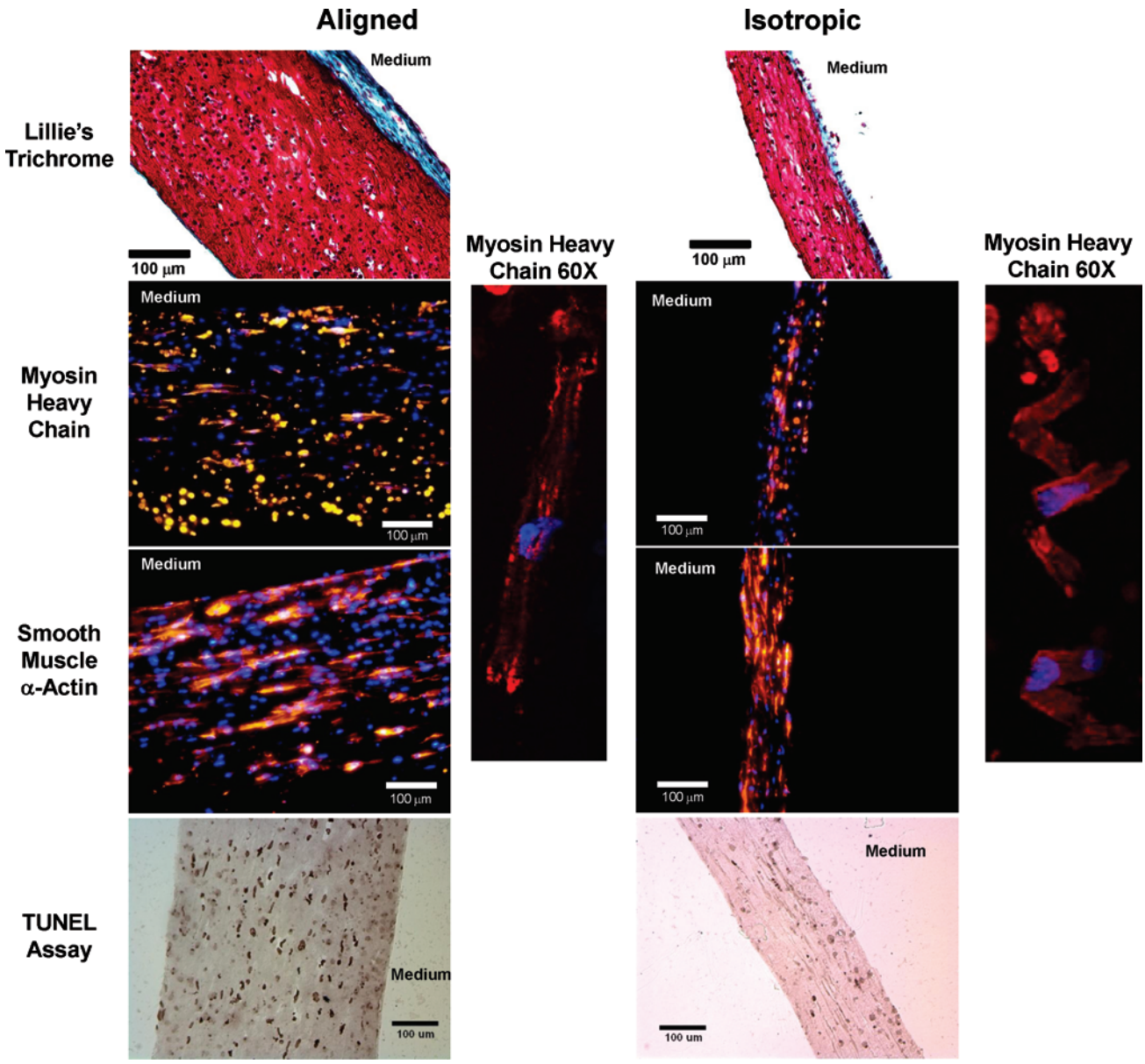

FIG. 2. Representative histological sections imaged at 10× for aligned and isotropic constructs. Constructs were stained with Lillie's Trichrome stain for matrix components (top row), and antibodies for myosin heavy chain (red stain, second row) and α-smooth muscle actin (red, third row). Note the inset of myosin heavy chain staining at 60× showing myosin fiber development and cross-striation typical of native myocytes (right of second and third rows). In addition, a TUNEL assay was conducted to assess apoptotic cells in aligned and isotropic constructs (bottom row). Note that TUNEL-positive nuclei stain dark brown or black to indicate apoptotic cells. Blue represents a DAPI counterstain for cell nuclei in the middle two rows. The surface in contact with the culture medium is noted for each image. In addition, the blue-green color of collagen stained in the trichrome stain is labeled in these images for both construct types. Color images available online at www.liebertonline.com/ten.

transport. Recent work by Radisic and colleagues has shown improved viability of myocytes with perfusion culture as well as the use of synthetic oxygen carriers.[24] Potential future studies with the ME system could involve methods for improving oxygen and nutrient transport to the constructs to enhance viability.

Another interesting result from the cell quantification was that the isotropic MEs contained significantly more cells than the aligned MEs. It is likely that the increased thickness of the aligned MEs resulted in reduced diffusion of oxygen and other nutrients into the center of the construct. This is supported by estimates in the literature that have determined that the diffusion limit of oxygen in engineered tissue is between 100–200 μm.[3,25] Further study of the histological images shows a decrease in cellularity (less DAPI-positive cells) near the surface of the aligned constructs that was in contact with the mandrel (middle rows, Fig. 2). The hypothesis that final cell number is related to the differences in geometry is further supported by the results from the TUNEL assay (bottom row, Fig. 2), which show an increased

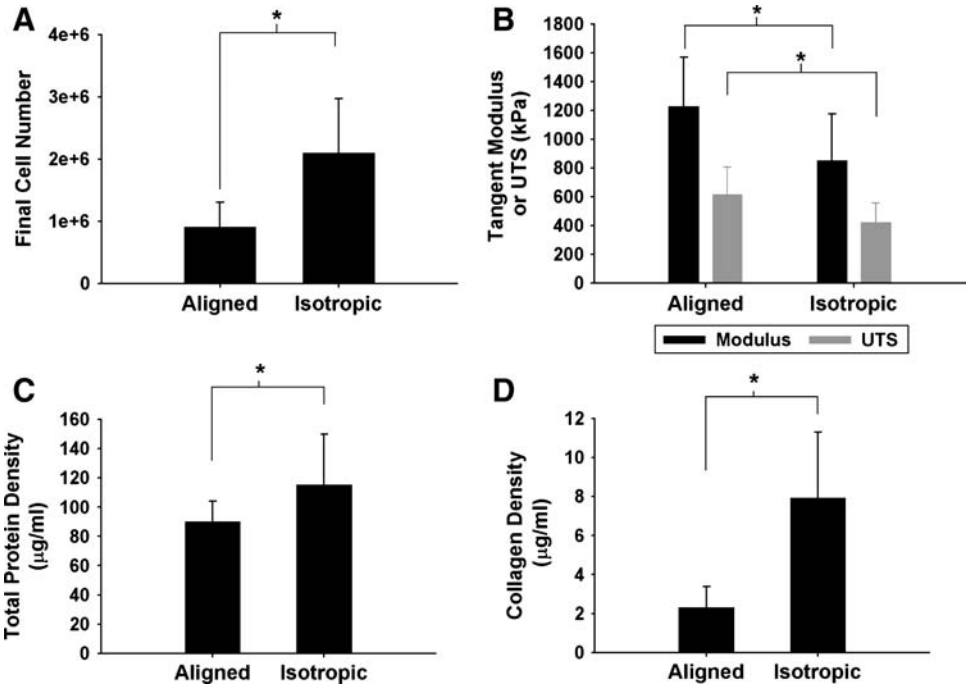

FIG. 3. (**A**) Final cell number in millions for aligned and isotropic constructs after 14 days in culture. Note that the isotropic constructs have almost twice as many cells remaining after 14 days. (**B**) Passive mechanical properties (modulus and UTS) for aligned and isotropic constructs after 14 days in culture. Total protein density (**C**) and collagen density (**D**) after 14 days in culture for aligned and isotropic constructs. Note that the isotropic constructs have higher total protein and collagen densities than the aligned constructs. $^*p < 0.05$ ($n = 14$ for all groups). UTS, ultimate tensile strength.

amount of apoptotic cells (dark brown/black nuclei) in the aligned constructs as compared to the isotropic constructs. It is also important to note that the final cell concentration of the isotropic constructs was around 1×10^8 cells/cm^3, approaching that of native tissue—5×10^8 cells/cm^3.[26] The aligned constructs had a significantly lower final cell concentration (0.46×10^8 cells/cm^3) due to the lower final cell number. Finally, quantification of the percentage of myocytes after 2 weeks in culture via FACS analysis showed that MHC-positive cells accounted for $54.6 \pm 8.4\%$ of the aligned constructs' cells and $33.0 \pm 6.5\%$ for isotropic constructs' cells ($p < 0.01$), as compared to 50% of the native neonatal rat heart.[27] The lower myocyte percentage in isotropic constructs, coupled with their increased cell number, implies that there is some proliferation of the cardiac fibroblasts in the isotropic case. Future studies will investigate the alterations in cellular composition with culture time to determine if this is the case.

Biochemical analysis revealed that both total protein density and collagen density were higher in isotropic constructs as compared to aligned constructs (Fig. 3C, D). However, when normalizing collagen density by final cell concentration, the isotropic and aligned constructs had similar values (81.3 ± 42.2 pg/cell for isotropic vs. 62.3 ± 27.8 pg/cell for aligned, $p = 0.18$), indicating that the larger collagen density in isotropic constructs after 2 weeks in culture was a result of the higher cell concentration. Regarding the difference in total protein density, it is important to note that our method for determining total protein includes collagen and the protein content of the cells themselves. Previous unpublished experiments from our lab have determined that the cellular contribution to total protein is approximately 220 μg/million cells. If we recalculate the final total protein per construct after removing the contribution of cells and the collagen content then the difference between construct types is ablated (1473.7 ± 265.6 μg for isotropic vs.

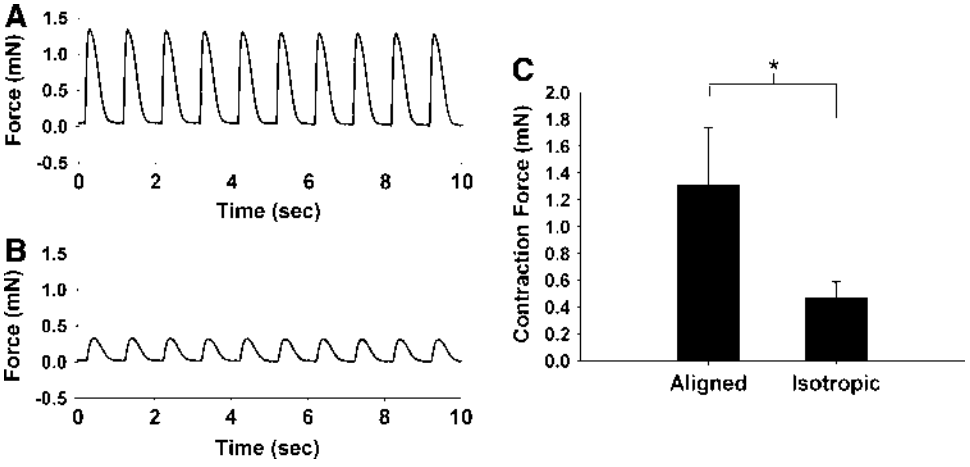

FIG. 4. Representative force traces during 1 Hz pacing versus time plots for an aligned (**A**) and an isotropic (**B**) construct. (**C**) Pooled twitch force data for 14-day-old aligned (left) and isotropic (right) constructs at 10 mN preload during 1 Hz pacing. $^*p < 0.05$ ($n = 14$ for both groups).

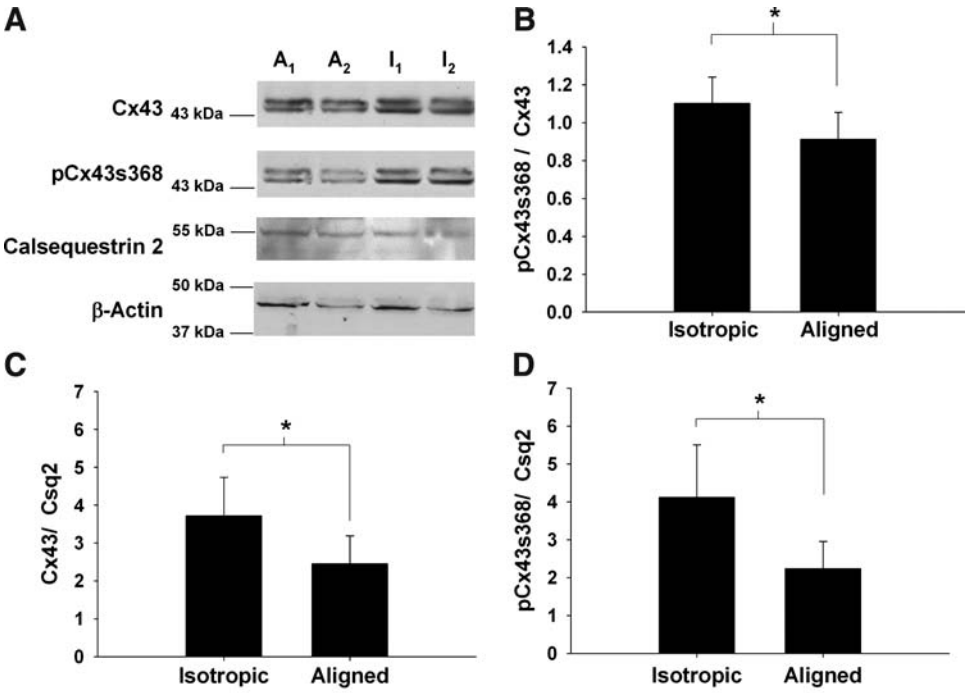

FIG. 5. (**A**) Representative Western blots for connexin 43 (Cx43), connexin 43 phosphorylated at serine 368 (pCx43s368), calsequestrin 2 (Csq2), and β-actin for two aligned (A_1, A_2) and two isotropic (I_1, I_2) constructs. (**B**) The ratio of pCx43s368 expression to Cx43 expression for aligned and isotropic constructs. (**C**) The ratio of Cx43 to Csq2 for aligned and isotropic constructs. (**D**) The ratio of pCx43s368 expression to Csq2 expression for aligned and isotropic constructs. $^*p < 0.05$ ($n = 6$ for all groups).

$1527.6 \pm 181.9\,\mu g$ for aligned, $p = 0.57$). Since the final volumes of the two construct types are not different, this implies that the increased protein density in the isotropic constructs is a result of the increased cellularity.

Figure 3B shows that aligned constructs exhibited higher modulus and UTS as compared to isotropic constructs ($p < 0.01$ for both). This result is somewhat expected since the mechanical properties were tested in the direction of alignment. However, the difference is even more notable considering the more than threefold higher collagen density in the isotropic constructs. The passive stiffness of native myocardium has been determined to be on the order of 50–100 kPa,[28,29] while measures of active stiffness are 10–20-fold larger.[30] The few reports of measured UTS of myocardium are in the range of 50–100 kPa[31,32] as compared to 400–600 kPa for our MEs. The values for the tangent modulus of our MEs (0.8–1.2 MPa) are much closer to those of active myocardium, and this is potentially a beneficial property. Infarcts waste energy generated by healthy myocardium via stretching or bulging, and have the potential to fail catastrophically via rupture, especially during the first week postinfarct.[33] The supraphysiologic UTS of our MEs could be critical in preventing rupture of the infarct during systole post-implantation. In addition, since the cells will be able to remodel the fibrin gel and deposit further ECM, it is likely that the mechanical properties will change post-implant in response to the milieu of the native heart during normal physiologic function.

Both aligned and isotropic constructs were contractile both spontaneously (2–3 Hz) as well as under general field stimulation (see Supplemental Video). Aligned constructs had a 181% higher twitch force than isotropic constructs ($p < 10^{-5}$). One possible reason for the higher twitch force could be purely geometrical: the twitch force is measured in the direction that the cells were aligned. However, in the isotropic case, there is no alignment; therefore, while cells that are perpendicular to the measurement direction may be contracting, their contraction did not contribute to the measured twitch force. To rule out this trivial explanation, the twitch force for an aligned construct was simulated from the isotropic data as follows: an average twitch force per cell was estimated for the final number of myocytes based on knowing the final cell number of the isotropic constructs (Fig. 3A) and the percentage of myocytes after 2 weeks in culture (FACS analysis); assuming a random of orientation of these cells; and then determining the measured twitch force if all of these cells were perfectly aligned in the measurement direction was calculated. The resulting simulated values, equal to normalization of the twitch force by cosine $(45^\circ) = \sqrt{2}/2$ (average angle of a random distribution between 0°

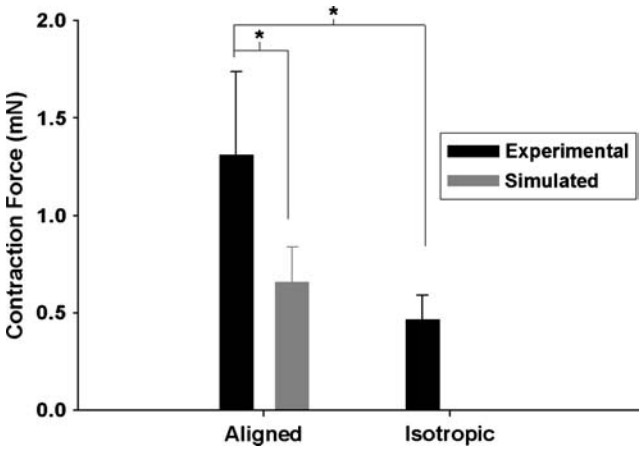

FIG. 6. Twitch force data for experimental data from aligned and isotropic constructs as well as aligned constructs simulated from isotropic data (see text). $^*p < 0.05$ ($n = 14$ for all groups).

and 90° is 45°), are shown in Figure 6. While there was an increase with simulated alignment, it is important to note that the values were still 50% less than those measured for the aligned constructs ($p < 0.0001$). These results suggest that cell-induced alignment of the ME imparts an increase in twitch force greater than merely aligning the cells in the direction of force measurement. Our hypothesis was that this was due to more gap junction formation and/or better organization and function of gap junctions resulting in better cellular communication.

To evaluate the cellular communication hypothesis, expression of Cx43, pCx43s368, and Csq2 was evaluated via Western blot (Fig. 5A). Phosphorylation of Cx43 can occur at multiple sites and has been implicated in the regulation of gap junctional communication at several stages of the connexin life cycle, including trafficking, assembly/disassembly, and degradation.[34] Studies have shown that the phosphorylation event pCx43s368 is increased in ischemic myocardium and targets the respective molecule for either intracellular translocation or degradation by the ubiquitin proteasome system[32] and may also reduce gap junction conductivity.[35] These studies indicate that pCx43s368 represents a less functional form of Cx43. The results presented in Figure 5B show that there was a greater percentage of pCx43s368 in isotropic as compared to aligned constructs ($p < 0.01$). Further, the Western blot analysis of Cx43/Csq2 (Fig. 5C) shows that the isotropic constructs had a greater expression of Cx43 per myocyte ($p < 0.04$); however, this increased expression is likely due to a greater expression of pCx43s368 as measured by significantly higher pCx43s368/Csq2 (Fig. 5D, $p < 0.02$). These data support the hypothesis that the improved twitch force of the aligned constructs is related to increased gap junction function. It is interesting to note that β-actin expression appeared different in different constructs of each type even with equal loading of the lanes according to the BCA assay. One reason for this would be a difference in β-actin expression for the different cell types in our construct (myocytes, fibroblasts). This difference, coupled with a difference in the ratio of these cell types in each construct, would result in the appearance of unequal loading of a gel. However, since the expression data in this manuscript are presented as ratios of expression of one protein to another for the same construct, any differences in total protein per lane are accounted for and this concern can be neglected. Future studies will be performed to evaluate Cx43 phosphorylation associated with other specific residues, differences in gap junction formation/localization (via imaging), as well as the differences in conduction velocity of the constructs using optical techniques (voltage sensitive dye and intracellular calcium imaging) to verify improved communication.

While these results indicate that gap junctions may be playing a role in the increased twitch force of the aligned MEs, there are other potential mechanisms that could be contributing to the measured difference in twitch force. One explanation would be a difference in how efficiently the force is transferred from the myocytes to the matrix between aligned and isotropic constructs. It is possible that the lack of ECM fiber alignment of the isotropic constructs would result in greater frictional losses in the transfer of the twitch force from the myocytes to the ECM. For example, some of the force generated by the myocytes could go to reorienting the isotropic fibers and not generating fiber tension, resulting in a lower measured force. Another explanation could be related to the matrix composition and the integrins expressed by the myocytes. The constructs are composed of mostly fibrin, an ECM protein not normally found in very high concentrations within myocardium. When entrapped in this matrix, myocytes may exhibit changes in their integrin expression. Alterations in integrin expression have been implicated in hypertrophy[36] as well as arrhythmias induced by loss of cellular mechanical coupling.[37,38] Future studies will investigate this as a potential mechanism by studying integrin expression in the MEs.

Finally, it is important to note that the twitch force values obtained for both groups are within the range of 0.2–1.5 mN previously published for contraction of engineered myocardium.[39] However, while these are appreciable twitch forces, they are still far below the values generated by native tissue. Thin muscle strips from rats devoid of core necrosis are capable of generating contractile stresses of up to 56 mN/mm^2.[40] Converting our data to contractile stress based on the size of our constructs results in values of 1.7–1.8 mN/mm^2 for aligned constructs. One important difference between the MEs and native tissue is that myocytes in native tissue make up approximately 30% of the cellular population and approximately 70–80% of the tissue volume.[41] Histological staining of our MEs suggests that even though myocytes made up 33–55% of the population of cells, they accounted for only 20–30% of the final cross-sectional area of the MEs, likely the result of both decreased viability and the lack of myocyte hypertrophy seen in native tissue. Even if the aligned MEs had the same cross-sectional area of muscle as native tissue, their contractile stress would be 4.0–7.2 mN/mm^2, still an order of magnitude below the native tissue. This difference could be further decreased by increasing functionality via alterations in isolation and culture conditions, including medium perfusion[24] and electrical stimulation.[5]

In summary, the creation of an ME graft *in vitro* represents a high-potential therapy for the repair of the heart post-myocardial infarction. Twitch force was significantly higher in aligned MEs as compared to isotropic MEs, and simulations suggest that this improvement is greater than what would be expected from merely aligning all of the cells in the isotropic MEs in the force measurement direction. Our hypothesis was that this extra improvement in twitch force was the result of improved gap junction formation and/or function in the aligned constructs. Western blot analysis of Cx43 and pCx43s368 expression showed a decrease in the less functional pCx43s368 in the aligned constructs. Further studies are needed to expand upon these results as well as correlate them with assessments of gap junction function via optical measures of conduction. Regardless of the specific mechanism, these results further underscore the importance of recapitulating the anisotropy of the native tissue in the creation of engineered myocardium *in vitro* for implantation *in vivo*.

Acknowledgments

The authors would like to acknowledge Stephen Stephens for technical assistance. This work was funded by the Institute for Engineering in Medicine at the University of Minnesota (R.T.T.), as well as an individual postdoctoral

fellowship from the National Heart, Lung, and Blood Institute (L.D.B.).

Disclosure Statement

No competing financial interests exist.

References

1. Hoyert, D.L., Heron, M.P., Murphy, S.L., and Kung, H.C. Deaths: final data for 2003. Natl Vital Stat Rep **54,** 1, 2006.
2. Miniati, D.N., and Robbins, R.C. Heart transplantation: a thirty-year perspective. Annu Rev Med **53,** 189, 2002.
3. Bursac, N., Papadaki, M., Cohen, R.J., Schoen, F.J., Eisenberg, S.R., Carrier, R., Vunjak-Novakovic, G., and Freed, L.E. Cardiac muscle tissue engineering: toward an *in vitro* model for electrophysiological studies. Am J Physiol **277,** H433, 1999.
4. Leor, J., Aboulafia-Etzion, S., Dar, A., Shapiro, L., Barbash, I.M., Battler, A., Granot, Y., and Cohen, S. Bioengineered cardiac grafts: a new approach to repair the infarcted myocardium? Circulation **102,** III56, 2000.
5. Radisic, M., Park, H., Shing, H., Consi, T., Schoen, F.J., Langer, R., Freed, L.E., and Vunjak-Novakovic, G. Functional assembly of engineered myocardium by electrical stimulation of cardiac myocytes cultured on scaffolds. Proc Natl Acad Sci USA **101,** 18129, 2004.
6. Nichol, J.W., Engelmayr, G.C., Jr., Cheng, M., and Freed, L.E. Co-culture induces alignment in engineered cardiac constructs via MMP-2 expression. Biochem Biophys Res Commun **373,** 360, 2008.
7. Shimizu, T., Yamato, M., Isoi, Y., Akutsu, T., Setomaru, T., Abe, K., Kikuchi, A., Umezu, M., and Okano, T. Fabrication of pulsatile cardiac tissue grafts using a novel 3-dimensional cell sheet manipulation technique and temperature-responsive cell culture surfaces. Circ Res **90,** e40, 2002.
8. Zimmermann, W.H., Schneiderbanger, K., Schubert, P., Didie, M., Munzel, F., Heubach, J.F., Kostin, S., Neuhuber, W.L., and Eschenhagen, T. Tissue engineering of a differentiated cardiac muscle construct. Circ Res **90,** 223, 2002.
9. Huang, Y.C., Khait, L., and Birla, R.K. Contractile three-dimensional bioengineered heart muscle for myocardial regeneration. J Biomed Mater Res A **80,** 719, 2007.
10. LeGrice, I.J., Takayama, Y., and Covell, J.W. Transverse shear along myocardial cleavage planes provides a mechanism for normal systolic wall thickening. Circ Res **77,** 182, 1995.
11. Costa, K.D., Takayama, Y., McCulloch, A.D., and Covell, J.W. Laminar fiber architecture and three-dimensional systolic mechanics in canine ventricular myocardium. Am J Physiol **276,** H595, 1999.
12. Bursac, N., Loo, Y., Leong, K., and Tung, L. Novel anisotropic engineered cardiac tissues: studies of electrical propagation. Biochem Biophys Res Commun **361,** 847, 2007.
13. Costa, K.D., Lee, E.J., and Holmes, J.W. Creating alignment and anisotropy in engineered heart tissue: role of boundary conditions in a model three-dimensional culture system. Tissue Eng **9,** 567, 2003.
14. Black, L.D., Meyers, J.D., Shvelidze, J., and Tranquillo, R.T. Development of a functional myocardial-equivalent based on cell-remodeled fibrin gel. Tissue Engineering and Regenerative Medicine International Society—North American Chapter Meeting. Toronto, Ontario, Canada: Tissue Engineering, 2006.
15. Grassl, E.D., Oegema, T.R., and Tranquillo, R.T. Fibrin as an alternative biopolymer to type-I collagen for the fabrication of a media equivalent. J Biomed Mater Res **60,** 607, 2002.
16. Clark, R.A., Nielsen, L.D., Welch, M.P., and McPherson, J.M. Collagen matrices attenuate the collagen-synthetic response of cultured fibroblasts to TGF-beta. J Cell Sci **108 (Pt 3),** 1251, 1995.
17. Barocas, V.H., and Tranquillo, R.T. An anisotropic biphasic theory of tissue-equivalent mechanics: the interplay among cell traction, fibrillar network deformation, fibril alignment, and cell contact guidance. J Biomech Eng **119,** 137, 1997.
18. Grassl, E.D., Oegema, T.R., and Tranquillo, R.T. A fibrin-based arterial media equivalent. J Biomed Mater Res A **66,** 550, 2003.
19. Tower, T.T., and Tranquillo, R.T. Alignment maps of tissues: I. Microscopic elliptical polarimetry. Biophys J **81,** 2954, 2001.
20. Williams, C., Johnson, S.L., Robinson, P.S., and Tranquillo, R.T. Cell sourcing and culture conditions for fibrin-based valve constructs. Tissue Eng **12,** 1489, 2006.
21. Stegemann, H., and Stalder, K. Determination of hydroxyproline. Clin Chim Acta **18,** 267, 1967.
22. Starcher, B. A ninhydrin-based assay to quantitate the total protein content of tissue samples. Anal Biochem **292,** 125, 2001.
23. Syedain, Z.H., Weinberg, J.S., and Tranquillo, R.T. Cyclic distension of fibrin-based tissue constructs: evidence of adaptation during growth of engineered connective tissue. Proc Natl Acad Sci USA **105,** 6537, 2008.
24. Radisic, M., Park, H., Chen, F., Salazar-Lazzaro, J.E., Wang, Y., Dennis, R., Langer, R., Freed, L.E., and Vunjak-Novakovic, G. Biomimetic approach to cardiac tissue engineering: oxygen carriers and channeled scaffolds. Tissue Eng **12,** 2077, 2006.
25. Carrier, R.L., Papadaki, M., Rupnick, M., Schoen, F.J., Bursac, N., Langer, R., Freed, L.E., and Vunjak-Novakovic, G. Cardiac tissue engineering: cell seeding, cultivation parameters, and tissue construct characterization. Biotechnol Bioeng **64,** 580, 1999.
26. Mandarim-De-Lacerda, C.A., and Meirelles Pereira, L.M. Numerical density of cardiomyocytes in chronic nitric oxide synthesis inhibition. Pathobiology **68,** 36, 2000.
27. Naito, H., Melnychenko, I., Didie, M., Schneiderbanger, K., Schubert, P., Rosenkranz, S., Eschenhagen, T., and Zimmermann, W.H. Optimizing engineered heart tissue for therapeutic applications as surrogate heart muscle. Circulation **114,** I72, 2006.
28. Mirsky, I., and Parmley, W.W. Assessment of passive elastic stiffness for isolated heart muscle and the intact heart. Circ Res **33,** 233, 1973.
29. Jalil, J.E., Doering, C.W., Janicki, J.S., Pick, R., Shroff, S.G., and Weber, K.T. Fibrillar collagen and myocardial stiffness in the intact hypertrophied rat left ventricle. Circ Res **64,** 1041, 1989.
30. Phillips, C.A., and Petrofsky, J.S. Myocardial material mechanics: characteristic variation of the circumferential and longitudinal systolic moduli in left ventricular dysfunction. J Biomech **17,** 561, 1984.
31. Przyklenk, K., Connelly, C.M., McLaughlin, R.J., Kloner, R.A., and Apstein, C.S. Effect of myocyte necrosis on strength, strain, and stiffness of isolated myocardial strips. Am Heart J **114,** 1349, 1987.
32. Boublik, J., Park, H., Radisic, M., Tognana, E., Chen, F., Pei, M., Vunjak-Novakovic, G., and Freed, L.E. Mechanical

properties and remodeling of hybrid cardiac constructs made from heart cells, fibrin, and biodegradable, elastomeric knitted fabric. Tissue Eng **11,** 1122, 2005.
33. Holmes, J.W., Borg, T.K., and Covell, J.W. Structure and mechanics of healing myocardial infarcts. Annu Rev Biomed Eng **7,** 223, 2005.
34. Lampe, P.D., and Lau, A.F. The effects of connexin phosphorylation on gap junctional communication. Int J Biochem Cell Biol **36,** 1171, 2004.
35. Ek-Vitorin, J.F., King, T.J., Heyman, N.S., Lampe, P.D., and Burt, J.M. Selectivity of connexin 43 channels is regulated through protein kinase C-dependent phosphorylation. Circ Res **98,** 1498, 2006.
36. Ren, J., Avery, J., Zhao, H., Schneider, J.G., Ross, F.P., and Muslin, A.J. Beta3 integrin deficiency promotes cardiac hypertrophy and inflammation. J Mol Cell Cardiol **42,** 367, 2007.
37. Saffitz, J.E. Dependence of electrical coupling on mechanical coupling in cardiac myocytes: insights gained from cardiomyopathies caused by defects in cell-cell connections. Ann NY Acad Sci **1047,** 336, 2005.
38. Valencik, M.L., Zhang, D., Punske, B., Hu, P., McDonald, J.A., and Litwin, S.E. Integrin activation in the heart: a link between electrical and contractile dysfunction? Circ Res **99,** 1403, 2006.
39. Zimmermann, W.H., and Eschenhagen, T. Cardiac tissue engineering for replacement therapy. Heart Fail Rev **8,** 259, 2003.
40. Hasenfuss, G., Mulieri, L.A., Blanchard, E.M., Holubarsch, C., Leavitt, B.J., Ittleman, F., and Alpert, N.R. Energetics of isometric force development in control and volume-overload human myocardium. Comparison with animal species. Circ Res **68,** 836, 1991.
41. Engelmann, G.L., Vitullo, J.C., and Gerrity, R.G. Morphometric analysis of cardiac hypertrophy during development, maturation, and senescence in spontaneously hypertensive rats. Circ Res **60,** 487, 1987.

Address correspondence to:
Robert T. Tranquillo, Ph.D.
Department of Biomedical Engineering
University of Minnesota
7-105 NHH
312 Church St. S.E.
Minneapolis, MN 55455

E-mail: tranquillo@cems.umn.edu

Received: September 9, 2008
Accepted: April 1, 2009
Online Publication Date: May 20, 2009